High-Altitude Simulation Tests of the LOX/LH_2 Engine LE-5

Koji Yanagawa* and Toshihiko Fujita†
National Space Development Agency of Japan, Miyagi, Japan
Hiroshi Miyajima‡
National Aerospace Laboratory, Miyagi, Japan
and
Kenji Kishimoto§
Mitsubishi Heavy Industries Ltd., Nagoya, Japan

The LE-5, under development since 1977 to power the second stage of the next Japanese launch vehicle, is an oxygen/hydrogen gas generator cycle engine with a thrust of 10.5 tonf at a chamber pressure of 36.8 kgf/cm^2 and a 140:1 area ratio nozzle. Flight-type engine tests were conducted under simulated altitude conditions. Engine specific impulse at a mixture ratio of 5.5 reached 448 s. The engine started smoothly and reliably with the tank head, fuel bleed start. Problems due to ice formation were solved by purges and heating.

Nomenclature

AT = auxiliary turbine
BFV = fuel turbopump bearing valve
BLV = LOX turbopump bearing valve
E/G = engine
ESV = engine start valve
FCV = fuel chill-down valve
FTP = fuel turbopump
GFV = gas generator fuel valve
GFPV = gas generator fuel purge valve
GG = gas generator
GHe = gaseous helium
GH_2 = gaseous hydrogen
GIG = gas generator igniter
GIV = gas generator igniter valves
GLV = gas generator LOX value
HE = heat exchanger
LCV = LOX chill-down valve
LH_2 = liquid hydrogen
LOX = liquid oxygen
LTP = LOX turbopump
MC = main combustion chamber
MFV = main fuel valve
MIG = main chamber igniter
MIV = main chamber igniter valves
MILV = main chamber igniter LOX valve
MLV = main LOX valve
NE = nozzle extension
SELI = second-stage-engine-lock-in signal
S/N = serial number

Introduction

THE next Japanese launch vehicle, named H-1, has been designed to place a 550-kg payload into geostationary orbit. The second-stage engine, LE-5 is an oxygen/hydrogen gas generator cycle engine with a thrust of 10.5 tonf at a chamber pressure of 36.8 kgf/cm^2 abs. A new start-up method, coolant bleed start, is employed. Although the coolant bleed cycle concept has been recognized for decades,[1] apparently, this is the first actual application of the cycle to start a gas generator cycle engine. Another distinctive feature of the LE-5 is its 140:1 area ratio nozzle. To the authors' knowledge, no flight engine of this thrust class has ever employed such a large area ratio nozzle.

The LE-5 has been under development since 1977. It was developed in three phases: design feasibility, design verification, and qualification phases. Figure 1 shows the planned and actual number of firing tests and the accumulated duration. During the design feasibility phase, prototype engine tests at sea level verified that the engine's performance met the required specifications.[2,3]

The design verification phase was successfully completed in March 1984. During this phase, four flight-type engines underwent altitude simulation firing tests and one engine underwent sea-level firing tests. This paper describes the altitude performance characteristics and the solution of various problems encountered therein.

Engine System Features

Table 1 shows the engine's major characteristics. To meet the H-I second-stage specifications, a flight burn duration of 370 s with 10,500±350 kgf in thrust and propellant mixture ration of 5.5±0.11 is required. Restart capability is required for some missions. The engine is illustrated in Fig. 2 and a schematic diagram is shown in Fig. 3.

Liquid hydrogen from the propellant tank is pressurized by a fuel turbopump, used as regenerative coolant of the combustion chamber section up to a nozzle area ratio of 8.5, and then ducted to the injector. Liquid oxygen is supplied directly to the injector from the oxygen turbopump outlet. Propellants tapped off at the outlet of the turbopumps are burned in the gas generator at a nominal mixture ratio of 0.85 and a chamber pressure of 26.4 kgf/cm^2 abs. Hot gases from the gas generator drive turbines of fuel and oxygen pumps in series and eventually are injected into the supersonic portion of the primary nozzle. The mass flow rate of the propellant supplied to the gas generator is about 1.8% of the total propellant flow rate.

A nozzle extension is attached to the chamber section at a nozzle area ratio of 8.5, making the overall area ratio 140:1. The nozzle extension is cooled by bypassing approximately 3% of the hydrogen from the outlet of the chamber coolant;

Received May 9, 1984; revision received Nov. 12, 1984.

*Assistant Senior Engineer, Kakuda Propulsion Center.
†Senior Engineer, Kakuda Propulsion Center.
‡Chief, Rocket Altitude Performance Section and Deputy Director, Kakuda Branch. Member AIAA.
§Senior Engineer, Liquid Rocket Engine Section.

the coolant is dumped through small supersonic nozzles at the primary nozzle exit.

Three orifices—the gas generator inlet orifices and the oxygen turbine bypass orifice—adjust thrust and mixture ratio.

Start Sequence

In gas generator cycle engines, it is usually necessary to apply start energy before the turbopumps accelerate to a sufficient level so that the gas generator bootstraps the turbines to a main-stage operational level. Start tanks or solid propellant turbine spinners are employed in upper stage engines.

In the present engine system, start energy is furnished by tank head hydrogen gasified in the chamber cooling passages. A typical start and shut-down sequence is shown in Fig. 4. The start sequence is as follows. Propellants chill down the two turbopumps and drain from the vehicle before the engine starts. Upon receipt of the ignition signal, torch igniters of the main chamber and gas generator are activated. After the engine start valve (ESV in Fig. 3) is opened, the main fuel valve (MFV) and main LOX valve (MLV) are opened serially. About 25% of the gaseous hydrogen from the outlet of the regenerative cooling passages goes through the start valve and drives the turbines of fuel and oxygen turbopumps in series and eventually is introduced into the nozzle. The remaining gaseous hydrogen is supplied to the injector and burns with liquid oxygen. The burned gases heat the wall of the chamber, which supplies energy to the increased amount of hydrogen. As the turbopump outlet pressures increase, the pressure and the amount of turbine drive hydrogen as well as those of the propellants supplied to the chamber increase, which in turn accelerates the turbopumps and the chamber pressure buildup. Reaching the programmed vehicle acceleration level, equivalent to 50% of engine thrust, the vehicle gives the second-stage engine lock in signal. Receiving this signal, the engine control box commands the ESV to close and the gas generator valves to open. After a short period of undershoot, the engine advances to a steady gas generator cycle.

Although similar to the expander start method, the main feature of the fuel bleed start method is its use of a partial amount of hydrogen to drive the turbines which then bleeds to the low-pressure nozzle section allowing a high-pressure ratio across the turbines. The major advantages of this start method are 1) since high-pressure starting devices such as start tanks or turbine spinners are unnecessary, the simple start system enables multiple restart, and 2) no chamber precooling is required.

Table 1 Major characteristics of the LE-5

Item	Nominal value
Thrust (vacuum), tonf	10.5
Combustion pressure (injector end), kgf/cm^{2}abs	36.8
Propellant mixture ratio	5.5
(restart mission)	5.6
Weight, kg	255
Length, m	2.65
Maximum diameter, m	1.65

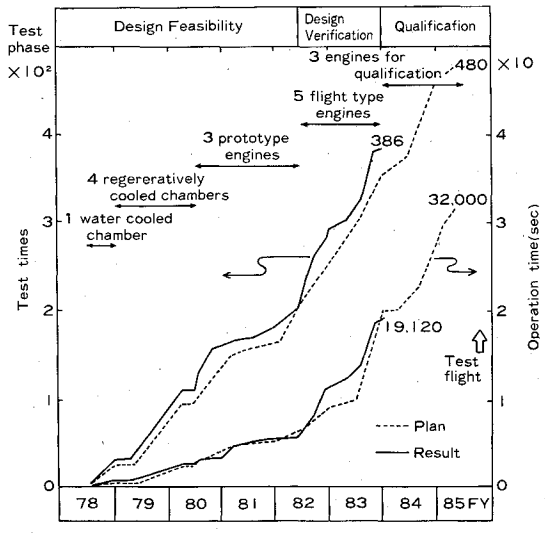

Fig. 1 Test summary.

Major Components

Thrust Chamber Assembly

A simplified drawing of the thrust chamber assembly is shown in Fig. 5. The injector is of a flat, Regismesh-faced, unbaffled design with a central hot gas port for the igniter. Two

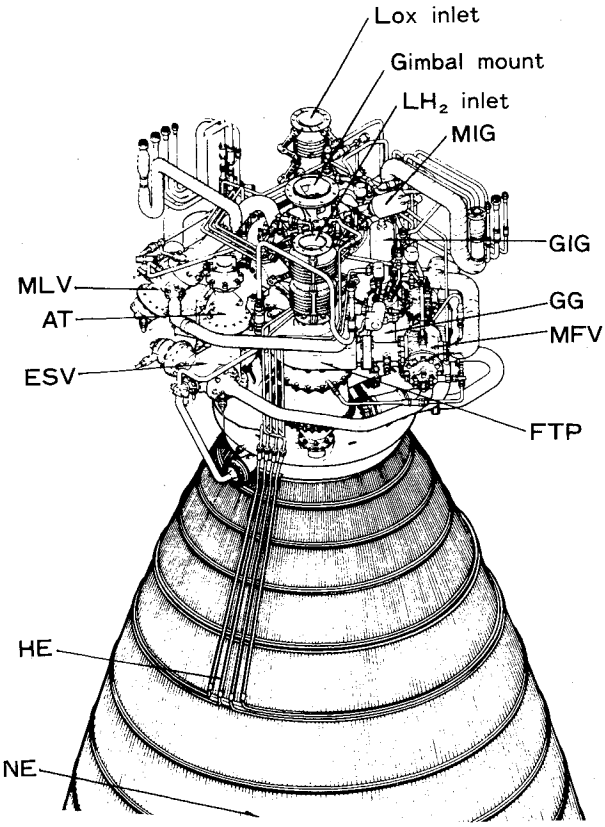

Fig. 2 General view of LE-5 engine.

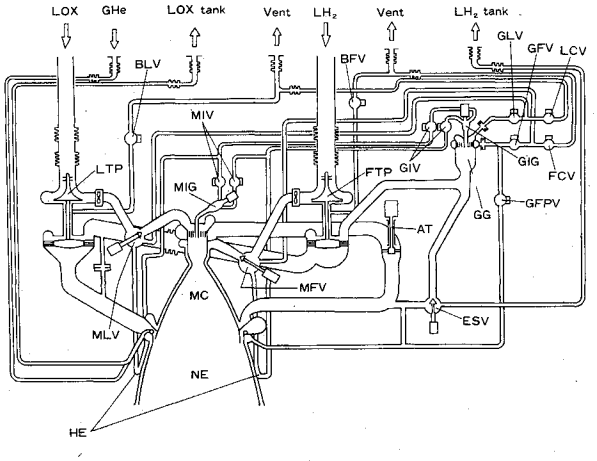

Fig. 3 Schematic diagram of engine system.

hundred and eight coaxial elements are uniformly distributed on a 240-mm-diam face plate. The injector element is designed so that the injection velocity ratio of hydrogen to oxygen is 20:1 at a hydrogen temperature of 140 K. A 1-diameter oxygen post recess and a 5-deg chamfer of the oxygen tube exit are also incorporated in the injector element design.

The major inner dimensions of the thrust chamber are shown in Fig. 5. The combustion chamber section, constructed of 240 brazed, double-tapered nickel tubes reinforced with a stainless steel outer shell, is terminated at the nozzle area ratio of 8.5:1 to facilitate sea level tests without nozzle extension. The nominal tube thickness is 0.3 mm. The chamber has 24 Helmholtz-type acoustic cavities at the injector, partially cooled regeneratively.

A simplified sketch of the turbine exhaust manifold and its injection nozzle is shown in detail A of Fig. 5 along with the other manifolds. Fifty discrete injection nozzles are on the base of a back step at the aft end of the chamber section. The geometry of the injection section is formed by cutting a step off the otherwise smooth optimum thrust contour. The nozzle extension was fabricated by brazing 650 stainless steel A-286 tapered tubes reinforced by 10 band rings. A small conical nozzle with an area ratio of 10:1 is inserted at the nozzle exit end of each tube.

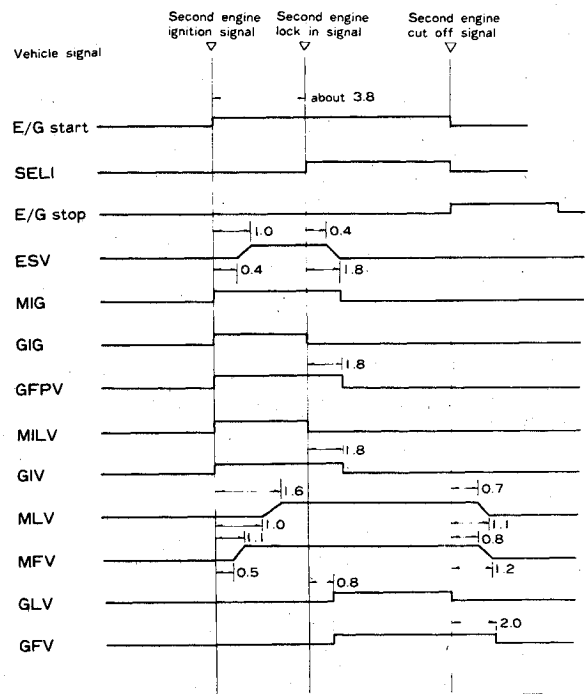

Fig. 4 Start and shutdown sequence (time intervals in seconds).

Turbopumps

Two independent turbopumps[4] for hydrogen and oxygen are employed. Both turbopumps are single-staged centrifugal pumps with inducers powered by a two-row, velocity-compounded impulse turbine.

Engine Start Valve

The engine start valve, a combined poppet and sliding slit cylinder valve design, is shown in Fig. 6. A cylinder valve function is required to control the flow rate of the hydrogen during the short interval after gas generator ignition to suppress thrust undershoot. The poppet provides complete shutoff.

Igniters

There are two igniters (one each for the main chamber and gas generator) which burn gaseous oxygen and gaseous hydrogen in the vacuum environment. Seven-meter-long tubes circumferentially attached to the nozzle extension gasify the propellants.

Test Facility

All of the tests presented here were conducted at the high-altitude test stand of the National Space Development Agency of Japan.[5] Basically, it consisted of a propellant supply

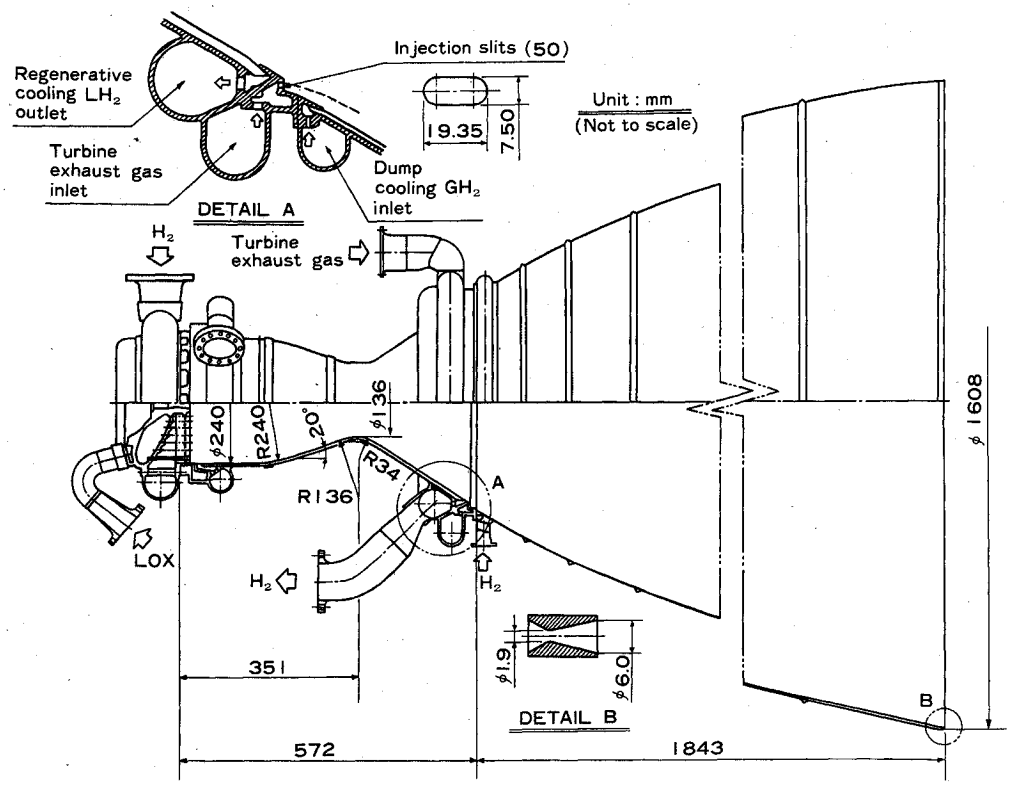

Fig. 5 Thrust chamber assembly.

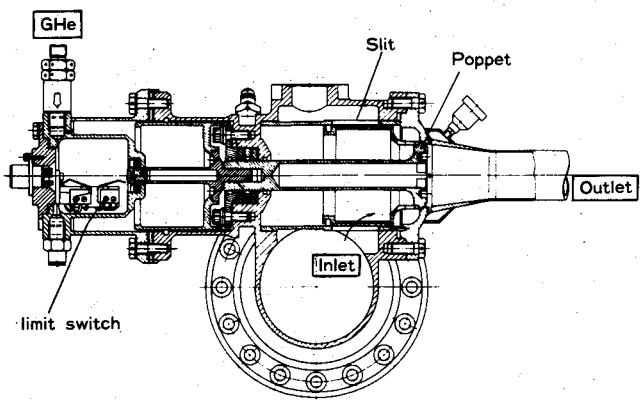

Fig. 6 Engine start valve.

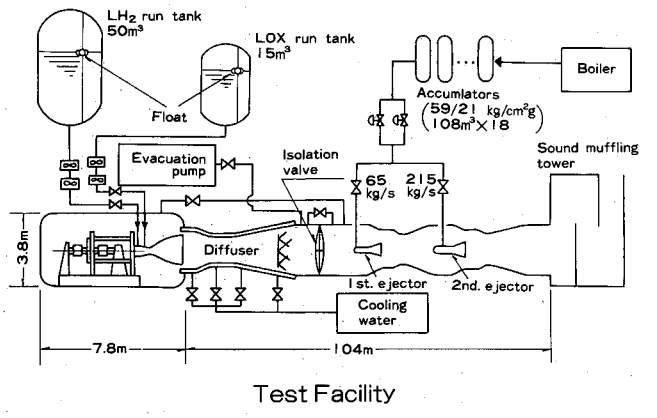

Fig. 7 Schematic diagram of test facility.

system, a thrust-measuring system in a vacuum capsule, and an exhaust system. A schematic diagram of the facility is shown in Fig. 7. The facility was designed for a maximum firing duration of 600 s. The exhaust system consisted of a second throat diffuser and a two-stage steam ejector. The capsule pressure was about 13 Torr before ignition and about 6 Torr during steady-state operation. The data acquisition of the engine and the facility was provided by a 221 channel digital system, a 28 channel analog recording system, and a 54 channel direct recording system. Twenty-four measured parameters were monitored in real time by the computer to generate emergency facility or engine shutdown signals.

Table 2 shows the estimated precision of the measured parameters in a steady state. The term precision is used here to represent an overall measurement uncertainty when every unknown bias which could not be elimated by calibration is assumed to be zero. The influence coefficient method was employed throughout for the propagation of measurement errors to the precision of the engine parameters. The most important single parameter is the vacuum specific impulse which depends on measured thrust, mass flow rate of propellants, capsule pressure, and nozzle exit area. The last two items did not contribute to the precision of vacuum specific impulse since the capsule pressure was sufficiently low. The estimated precision of the thrust and propellant flow rate will be discussed in the next subsections.

Thrust-Measuring System

The axial thrust was measured by a load cell in a tension mode. The thrust mount and thrust transmission structure were suspended from two support frames by plate springs to allow only axial displacement. The measurement load cell was calibrated in place by an hydraulically powered worm screw. Universal flexures attached to both ends of a load cell reduced

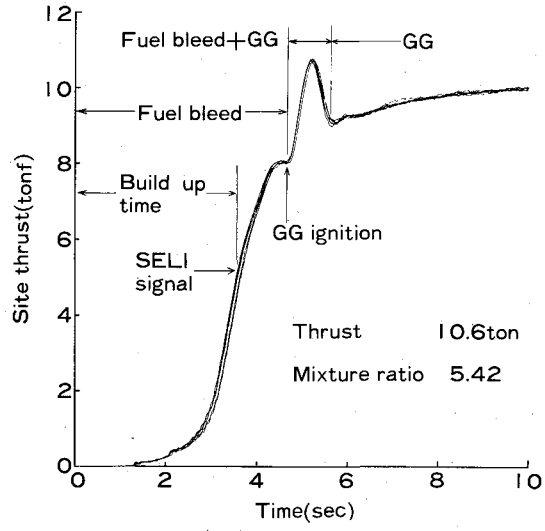

Fig. 8 Typical thrust vs time curve and its reproducibility.

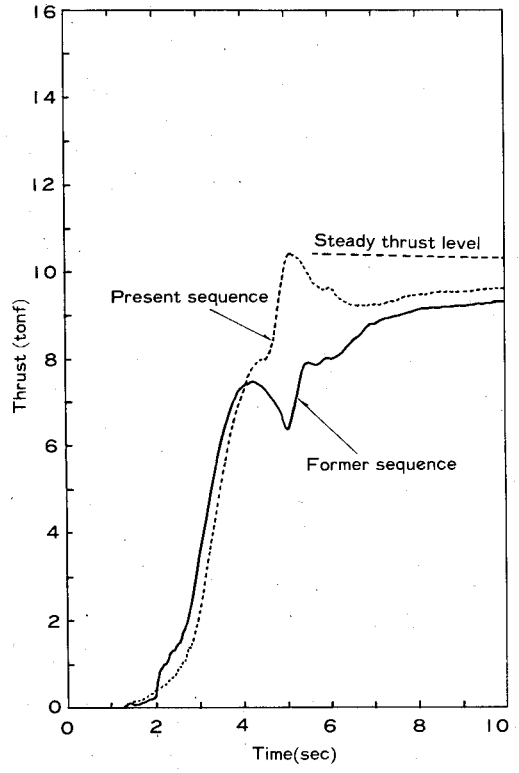

Fig. 9 Comparison of thrust curves between present and former sequences.

interaction with forces other than axial. The standard load cell was calibrated periodically with dead weights which are traceable to the National Research Laboratory of Meterology (NRLM). The traceability constant was estimated to be 0.024%.

Thrust-measuring system calibration may be performed at vacuum as well as at sea level. No difference between the calibration constants of sea level and vaccum conditions was detected. A calibration test with cold propellant lines also indicated that the calibration constant did not change appreciably.

The load cell had two channels of strain gage output averaged in the measurement. The overall system precision per channel was determined to be 0.131% and the effect of dual measurements was taken into account to give a combined precision of the thrust measurement of 0.092%.

Table 2 Nominal operating conditions and estimated precision

Item	Nominal value	Precision, % of nominal
Capsule pressure, Torr	6.2	0.29
Vacuum thrust, tonf	10.5	0.09
LOX mass flow rate, kg/s	19.83	0.25
LH_2 mass flow rate, kg/s	3.61	0.26
Engine mixture ratio	5.5	0.36
Engine specific impulse, s	448.0	0.24

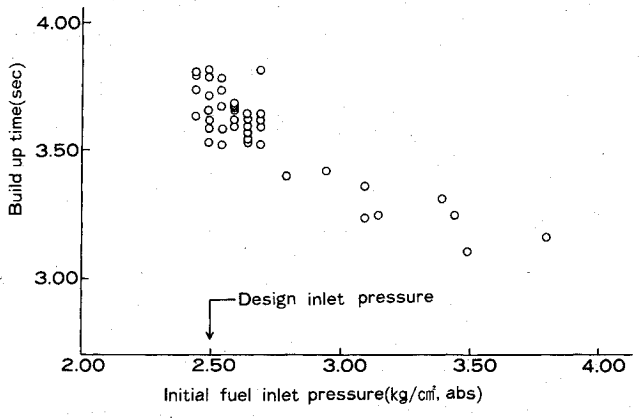

Fig. 10 Dependence of buildup time on fuel inlet pressure.

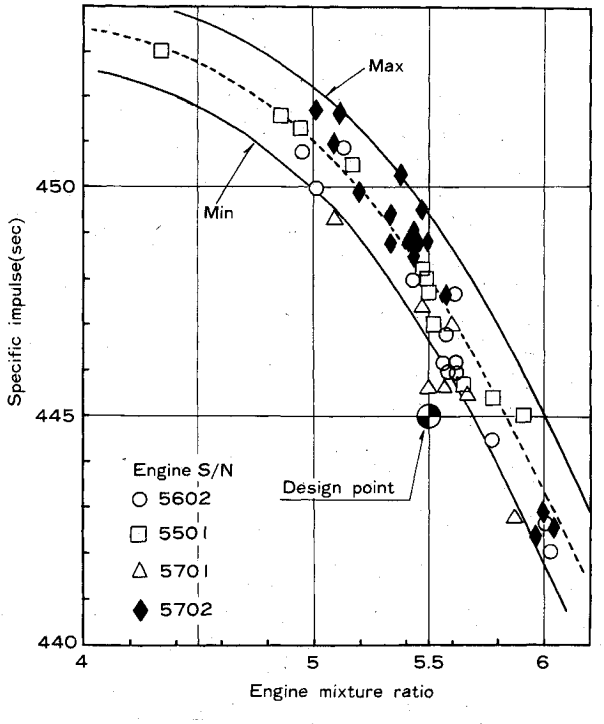

Fig. 11 Engine vacuum specific impulse.

Propellant Flow Rate Measurement

Two turbine flowmeters in series were used in each of the main propellant lines. The flowmeters were calibrated in place by cryogenic propellants in each long-duration firing test. The run tanks served as a volume calibration system as well as for propellant storage and supply. The insulated tanks has long cylindrical sections. Each tank has 22 reed switches housed in a pipe at different vertical locations and a lightweight float assembly which moved along the pipe. At the center of the float assembly was a magnet ring through which the tube passed. The magnet activiated the switches with a decrease of liquid level.[6]

Level-volume calibration of the propellant tanks was conducted using water with standard volume measuring tanks traceable to NRLM. The precision of increment volume measurement between the adjacent switches never exceeded 0.09% after correction for cryogenic temperatures and tank pressures.

As mentioned previously, turbine flowmeters were calibrated in each long-duration (370 s) firing test. The calibration constants were renewed periodically. The system precision per channel of volume flow measurement was estimated to be 0.299% for liquid hydrogen and 0.347% for liquid oxygen. The precision of mass flow rates was calculated by accounting for the precision of temperature and pressure measurements which were required to determine densities. Finally, the mass flow rate precision thus estimated was divided by $\sqrt{2}$ to account for dual measurement (see Table 2).

Test Results

Sixty eight altitude simulation tests on four engines accumulated a firing duraton of 6408 s.

Start Transient

Numerous computer simulations and sea level start tests were conducted to establish the fuel bleed start procedure. The initial step was to determine the timing sequence with reference to experimental thrust vs time curves using a poppet-type start valve. It was found that a substantial undershoot immediately after gas generator ignition was unavoidable even in the optimum valve timing sequences. This was due to the chilling of ducts and other hardware during the fuel bleed phase. The thrust undershoot was considered harmful due to possible flame out and diffuser breakdown in the high-altitude simulation tests.

In addition, it was anticipated and proved by tests that the slope of the thrust curve depended on the environmental pressure (vacuum or sea level) as well as the initial hydrogen tank pressure.

The following modification was made on the start system. First, the poppet-type start valve was replaced by one with a sliding slit cylinder mechanism (Fig. 6) to facilitate better control of the hydrogen flow rate during the short period after gas generator ignition. Second, instead of a predetermined time sequence, the gas generator valves were opened after sensing 50% of the steady main chamber pressure. Vehicle acceleration will be monitored in a flight to generate a second-stage engine lock in (SELI) signal. A typical thrust vs time curve in a low-pressure environment is shown in Fig. 8 to illustrate the sequence of events. A comparison of thrust curves between the present start system and the older one is shown in Fig. 9. It may be seen that the thrust undershoot was eliminated completely. Figure 8 also shows a degree of reproducibility for six thrust curves of an indentical engine with similar initial fuel inlet pressures. Although the thrust curves for different steady thrusts and mixture ratios did not coincide as precisely as those shown in Fig. 8, they were very close to each other before gas generator ignition.

Figure 10 shows the dependence of buildup time on the initial fuel inlet pressure. The buildup time is defined as the interval of time from the ignition signal to the instant 50% steady thrust is achieved (Fig. 8). The data shown in Fig. 10 are for three different engines. The buildup times for lower fuel inlet pressures were in the range of 3.5-3.8 s for a nominal initial inlet pressure of 2.5 kg/cm^2 abs. Such scattered data was primarily due to engine-to-engine variation and, to a lesser degree, variation of precooling and steady operating conditions.

Sea level, battleship propulsion system firing tests with an ejector to provide low pressure to the turbine exhaust have

shown that the start is smooth and reproducible at nominal inlet conditions. However, the buildup time for the battleship firing tests was 3.9 s on average, which was longer than that of the altitude simulation tests. The arrangement of propellant tanks was different from flight hardware for the altitude simulation test. The transient inlet pressures in the altitude tests were simulated by closing a bypass valve so that the initial and steady inlet pressures were close to flight values. Disturbances produced by the bypass valve closing were not eliminated completely. The difference of buildup times between battleship and altitude tests is presently attributed to be the result of these disturbances.

Engine Specific Impulse

Engine performances depended on firing time to a certain extent. The thrust was approximately 90% of the steady level after gas generator ignition and took more than 100 s to attain steady state. Mixture ratio converged to a constant value after about 40 s. Vacuum specific impulse generally attained a constant value after 40 s, except in a few cases where it increased continuously but slightly for the entire duration (370 s). For steady-state data, the average of 500 data points between 95 and 100 s was used for performance calculation. An exception is made for the earlier tests (engine serial Nos. 5602 and 5501) where firing duration in most tests was limited to 40 s. Here, the average of data between 35 and 40 s after ignition was used.

Figure 11 shows the steady vacuum specific impulses. Table 3 compares changes in thrust chamber components of each engine. Engines 5501 and 5702, whose chambers were constructed of Ni-200 tubes, showed a specific impulse gain of more than 2 s compared to engine 5602 whose chamber was constructed of stainless steel A-286 tubes. Heat transferred to the hydrogen coolant for the nickel chamber was 1.3 times that for the A-286 chamber. The specific impulse increase may be attributed to increased energy release efficiency due to the velocity ratio increase at the injector elements.

The specific impulses for an engine with LOX swirl injector (engine 5701) clearly were smaller than those of the other engines with nickel chambers. Swirlers were inserted into the LOX tubes of all elements except those at the outermost ring of the injector. It turned out that an inadequate design and insertion of the swirlers increased the pressure drop through the swirl elements. This, in turn, produced a substantial nonuniform mass and mixture ratio distribution over the injector and presumably reduced the delivered specific impulse.

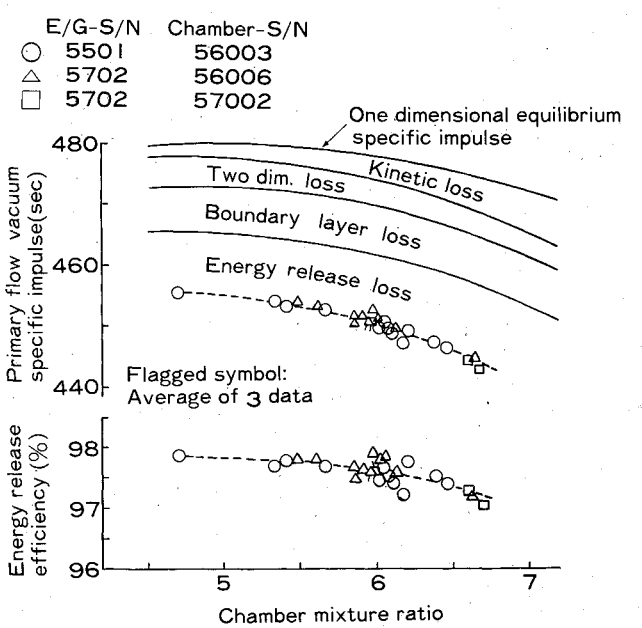

Fig. 12 Primary flow vacuum specific impulse.

The measured decrease in heat transfer to the hydrogen coolant substantiated this presumption.

The specific impulse of the present configuraion, i.e., with a standard injector and nickel chamber, is estimated to be 448 ± 1.1 s at a nominal mixture ratio of 5.5.

Figure 12 shows a degree of the injector energy release loss in addition to the various nozzle losses for the present thrust chamber configuration. In the estimation of the energy release efficiency, the primary flow specific impulse was first obtained by subtracting turbine exhaust and dump coolant contributions from the measured engine specific impulse by simple calculations; it was then divided by the calculated primary flow specific impulse with a perfect energy release.[7] It is seen from Fig. 12 that energy release efficiencies for different chambers and injectors of the same design do not differ appreciably. The energy release efficiency of the injector is presently estimated to be 97.6% at a chamber mixture ratio of 6.1 which corresponds to an engine mixture ratio of 5.5. The data for engines with a combustion chamber section constructed of A-286 material and a LOX swirl injector were not included in Fig. 12 because they do not represent the present configuration.

Unsatisfactory Conditions and Corrective Actions

Main Chamber Tube Materials

The tube surface near the throat of the chamber, constructed of stainless steel A-286, sometimes eroded and developed cracks. Figure 13 shows a cutaway specimen of eroded and normal tubes. It was presumed that insufficient local cooling caused the erosion during the start and shutdown transient. A-286 material eventually was replaced by nickel (Ni-200). No erosion was observed thereafter.

Gas Generator Wall Burnout

One unexpected problem apparently was caused by the fuel bleed start. In one test, the gas generator wall near the injector eroded through to the outer surface. Failure was assumed to occur when cold hydrogen driving the turbopumps during the fuel bleed phase cooled the injector face of the gas generator and led to condensation and freezing of water from the igniter gases; consequently, ice formed around a coaxial injector element and deflected the jet toward the wall. Modification was made to allow helium and gasified hydrogen purges for oxygen and hydrogen passages, respectively, before gas generator ignition. After this corrective action, no anomaly occurred.

Ice Formation in the Igniters

During steady gas generator operation, in which its igniter was inactive, the throat of the igniter was blocked by ice on rare occasions. This led to restart failure and abort of restart tests. On another occasion, a hard start in the second ignition was observed due to oxidizer flow restriction at the main chamber igniter flow metering orifice. The following corrective actions were effective:

1) Application of a warm gaseous hydrogen purge to hydrogen lines from a heat exchanger around the nozzle extension after the igniters are turned off.

2) Installation of a heater for the oxygen line near the main igniter.

Table 3 Major change of thrust chamber components

Engine Serial No.	Injector	Chamber material	Nozzle tube thickness, mm
5602	Standard[a]	A-286	0.3
5501	Standard	Ni-200	0.3
5701	LOX swirl	Ni-200	0.25
5702	Standard	Ni-200	0.25

[a]Described in section on major components.

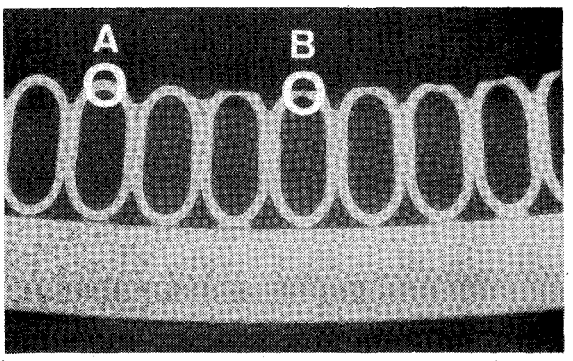

a)

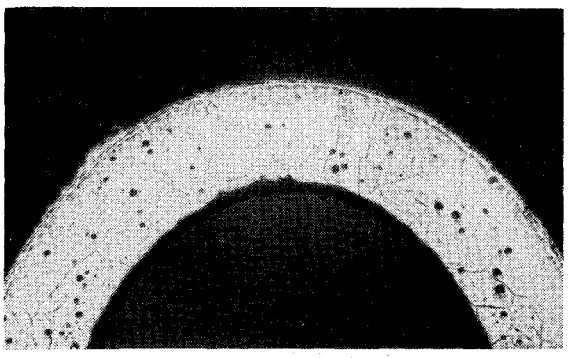

b)

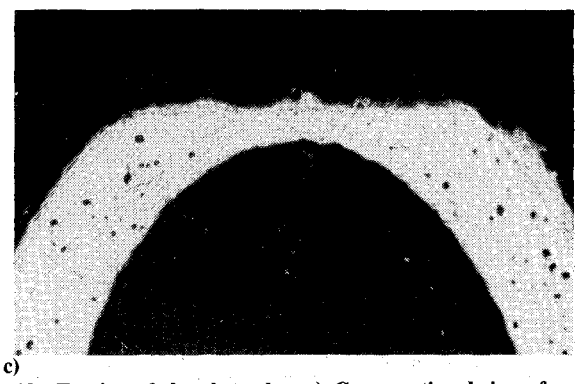

c)

Fig. 13 Erosion of chamber tube. a) Cross-sectional view of a main chamber. b) Portion bounded by circle A, normal tube. c) Portion bounded by circle B, eroded tube.

Concluding Remarks

Major conclusions drawn from the altitude simulation tests conducted during the design verification phase of the LE-5 engine development are as follows:

1) The engine started smoothly and reliably with the fuel bleed start.

2) A vacuum specific impulse of 448 s was demonstrated at an engine mixture ration of 5.5.

3) Problems due to ice formation, primarily related to reignition, were solved by purges and heating.

The design verification phase was completed successfully in March 1984, and will be followed by the qualification phase. The first flight is scheduled for February 1986.

Acknowledgments

The authors wish to express their gratitude to the technical staff of Ishikawajima Harima Heavy Industries Ltd., for their participation in the test series and assuming responsibility for the turbopumps and gas generators.

References

[1]Sutton, G.P. and Ross, D.M., *Rocket Propulsiton Elements,* John Wiley & Sons, New York, 1976, pp. 213-215.

[2]Makino, T., Fujita, T., Suzuki, A., Miyajima, H., Kuratani, K., and Tanatsugu, N., "Development Status of LE-5 Oxygen-Hydrogen Rocket Engine," Paper 82-352 presented at XXXIII IAF Congress, Paris, 1982.

[3]Hirata, K., Denda, Y., Yamada, A., Kochiyama, J., Fujita, T., and Katsuta, H., "Development Test of LE-5 Rocket Engine," *Proceedings of the 13th International Symposium on Space Technology and Science,* Tokyo, 1982, pp. 237-242.

[4]Kamijo, K., Sogame, E., and Okayasu, A., "Development of Liquid Oxygen and Hydrogen Turbopumps for the LE-5 Rocket Engine," *Journal of Spacecraft and Rockets,* Vol. 19, May-June 1982, pp. 226-131.

[5]Hashizume, H., Yamamoto, R., Sasaki, S., Takano, A., Kochiyama, J., Tamura, Y., and Sakazume, N., "Development of Facilities for LOX/LH_2 Rocket Propulsion System in NASDA," *Proceedings of the 13th International Symposium on Space Technology and Science,* Tokyo, 1982, pp. 353-358.

[6]Yanagawa, K., Fujita, T., Kikuchi, K., Kuzumaki, M., and Yamazaki, K., "Development of Cryogenic Liquid Level Gauge," *Proceedings of the 9th International Cryogenic Engineering Conference,* Kobe, Japan, May 1982. pp. 650-654.

[7]Miyajima, H., Nakahaski, K., Yanagawa, K., and Fujita, T., "Specific Impulse Analysis of the LE-5," AIAA Paper 84-1224, June 1984.